

# Physical modelling as a tool to improve our understanding of mechanisms of cave flow

R Castro *Universidad de Chile, Chile*

RE Gómez *Universidad de Concepción, Chile*

Á Pérez *Universidad de Chile, Chile*

## Abstract

*In block caving, gravity flow of broken ore has been studied using different tools, highlighting the application of scaled physical models, numerical modelling and field studies. These tools, with their advantages and disadvantages, have allowed different variables involved during ore draw to be studied. In this paper, we summarise years of physical experiments run in the Block Caving Laboratory to study different underground mining issues. In particular, experiments have been carried out to study fine material migration, induced stresses due to ore draw, secondary fragmentation, hang-ups formed on drawpoints, drawbell geometries, inrush of fines material, and ore extraction in mud conditions. The main significances, its impact and application, are discussed here. This work shows that physical modelling continues to be a powerful and useful tool to study gravity flow in block cave mines, allowing to understand diverse mine engineering problems and to be a practical input to calibrate complex numerical models.*

**Keywords:** *block caving, gravity flow, physical modelling, rock mechanics, underground mining*

## 1 Introduction

The granular material experiments through physical models have been used for years in different disciplines, such as pharmaceuticals, alimentary, geology, and mining (Bock & Prusek 2015; Killion 1985; Mahmoodi 2012). In mining, one of the first attempts was done by Kvapil (1965), who studied the gravity flow for cave mining. In cave mining, the main interests are related to the interaction between extraction zones for mine design, maximising ore recovery, waste/ore draw control, fine material migration, avoiding risk conditions due to stress concentration, air blast, mud-rushes and inrush of fines (Brown 2007; Laubscher 2000a; Susaeta 2004). Furthermore, the study of gravity flow helps to define production plans and estimate secondary fragmentation. Several studies have been developed through physical scaled models (e.g Castro 2007; Castro et al. 2020a; Castro et al. 2020b; Castro et al. 2022a; Castro et al. 2014; Gómez & Castro 2022a; Jenike et al. 1973; Kvapil 1965, 2008; Laubscher 1994; Sperl 2006), as well as field tests (e.g Brunton et al. 2016; Gustafsson 1998; Laubscher 1994; Power 2004; Steffen & Kuiper 2014; Viera & Diez 2014), and numerical models mainly using discrete element methods and cellular automata (e.g. Baxter 2012; Calderon et al. 2004; Castro et al. 2022b; Cleary & Sawley 2002; Gómez & Castro 2022b; Hancock 2013; Jolley 1968; Langston et al. 1995; Sun et al. 2019).

The numerical methods offer the advantage of being able to study problems and variables that are sometimes difficult to observe and control in physical or full-scale studies. As an example, with distinct element method (DEM) we can study stress chain and inter-particle interaction, modified material properties (such as: density, elastic modules, friction parameters), and nowadays realistic rock fragment shapes can be used (ESSS 2022; Michot-Roberto et al. 2021). Large-scale simulations have been developed in DEM using spherical particles (Hancock 2013; Pierce et al. 2017). However, long simulation times are required to simulate an entire block cave mine. Nevertheless, there are numerical tools that can be simulate the gravity flow in block cave mines quicker (Castro 2007; Castro et al. 2022b; Pierce 2009; Dassault Systèmes 2018).

The tools used to study gravity flow indicated above are used depending on the problem and the variables to analyse. In particular, this paper focuses on physical experiments carried out in the Block Caving Laboratory at the Universidad de Chile, to study problems related mainly to block caving methods. These studies have been developed at laboratory-scale, and in some cases, also have been compared with field data or used to calibrate numerical models.

## 2 Laboratory equipment

### 2.1 Physical models

The Block Caving Laboratory was founded in 2008 and is located at the Universidad de Chile. In the laboratory several mining studies mainly related to gravity flow have been developed. Here, physical models from 1:50 to 1:200 scale in 2D and 3D environments have been built using different granular materials such as gravel, sulphide ores, oxide ores, mortar, brick, gypsum and charcoal to represent different material properties. Gravity flow under confinement conditions has also been tested to replicate the overload of high broken columns. All these allow gravity flow of caving mining to be studied and contribute new knowledge of mine planning and design. Figure 1 summarises various physical models built and used in the laboratory.

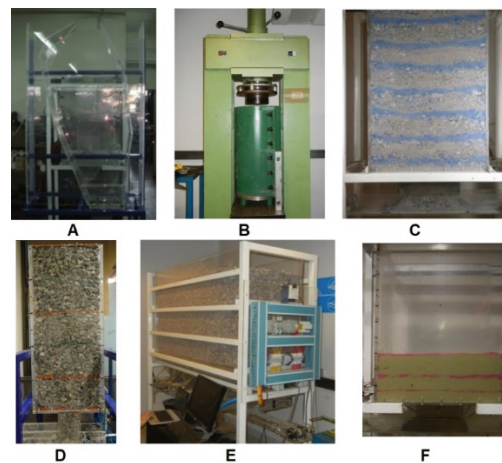


**Figure 1** Physical models of various gravity flow studies. (a) Fine material migration in a large stope; (b) Gravity flow under confined conditions; (c) Drawbell geometry influences on hang-ups; (d) Dozer extraction system; (e) Block caving continuous mining; (f) Proof model for mud extraction

Additionally, these physical models presented emulate ore extraction using different extraction systems. Dozer systems and scale buckets (emulating load–haul–dump (LHD) equipment) have been tested. Figure 2 shows both extraction systems used at laboratory-scale. These extraction systems are remote controlled or autonomous.

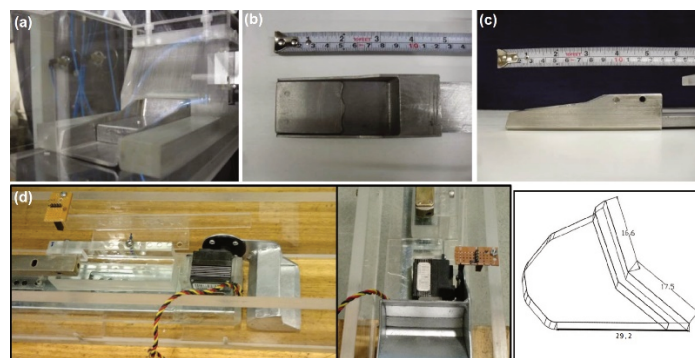


**Figure 2** Extraction system used in physical models. (a) Dozer equipment; (b–c) LHD equipment (Orellana 2012); (d) LHD and motors (Castro et al. 2020a)

## 2.2 Granular material characterisation

Several granular materials have been tested in gravity flow studies. However, gravel and ore (sulphides) are the most commonly used in the laboratory because they have properties similar to rocks in mining environments of block caving. Gravel rock is preferred mainly because it is accessible in the required fragment sizes, has high strength, and the expected density of Chilean mines. The main drawback of the gravel is its roundness. Ore fragments from Chilean mines are preferred because they have the mechanical rock properties required. The main drawbacks are its accessibility in the required quantities and that they must be fragmented to scale-fragment size.

The rock properties and characteristics to be determined depend on the test and variables under study. The real density, the bulk density (ASTM International 2002; ASTM International 2018), the moisture percent, the fragment size distribution, the rock fragment strength ( $IS_{50}$ ) (ASTM International 2008), the shear strength (ASTM D3080/D3080M 2011), the internal friction angle, and the shape factors (Cho et al. 2006) are mainly measured. In some studies, additional instruments such as the Abrams cone have been incorporated to determine the plasticity of wet granular material for mud rush studies (Castro et al. 2017; Vallejos et al. 2017).

## 2.3 Main variables analysed

In caving mining, the experiments using physical models have been largely used for the study of different variables. In some cases, based on the experimental setup and scopes, more than one variable can be studied. A summary of the main variables analysed using experiments in gravity flow studies follows:

- Flow zone geometries (extraction and movement zones; isolated and interactive draw).
- Mine structure geometries (drawbells, drawpoints, spacing, conventional LHD and dozer systems).
- Fine material migration.
- Undercut height.
- Stresses (vertical and horizontal in physical model boundaries).
- Rock fragmentation due to draw.
- Drawpoint/extraction system productivity.
- Hang-ups (coarse and cohesive arches).
- Mud extraction.

The flow zone geometries are measurement using markers inside the granular media (Figure 3a) and flow lines (Figure 3b). These markers are collected during draw experiments when they appear in drawpoints while the flow lines are measured throughout the experiment through the plexiglass walls.

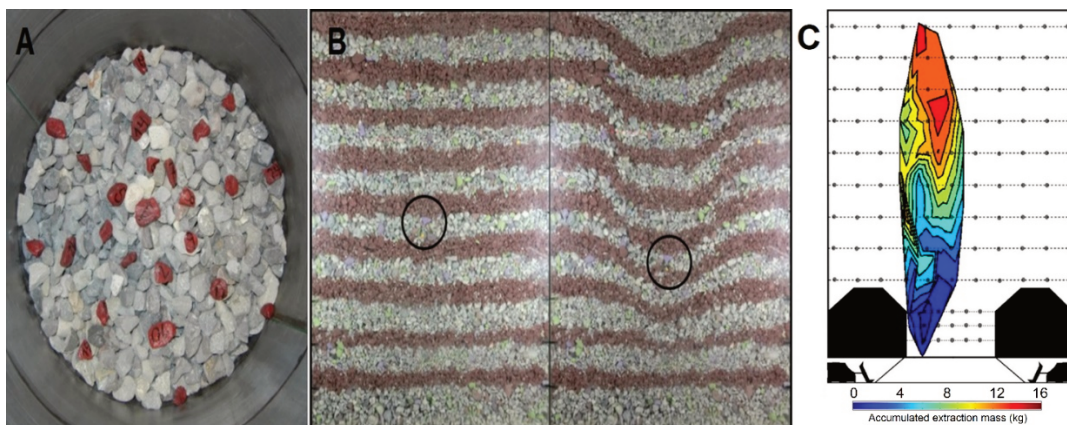


**Figure 3 Flow zone measurement. (a) Markers within granular material; (b) Flow lines in model boundaries; (c) Extraction zone identification built through marker recovery after draw**

Extraction and movement zones can be identified using markers in physical models. Then, ore recovery and the height of interaction between drawpoints can be determined. Additionally, these zones are influenced by the geometry of the mine’s structure. Different drawbell geometries have been tested as shown in Figure 4a.

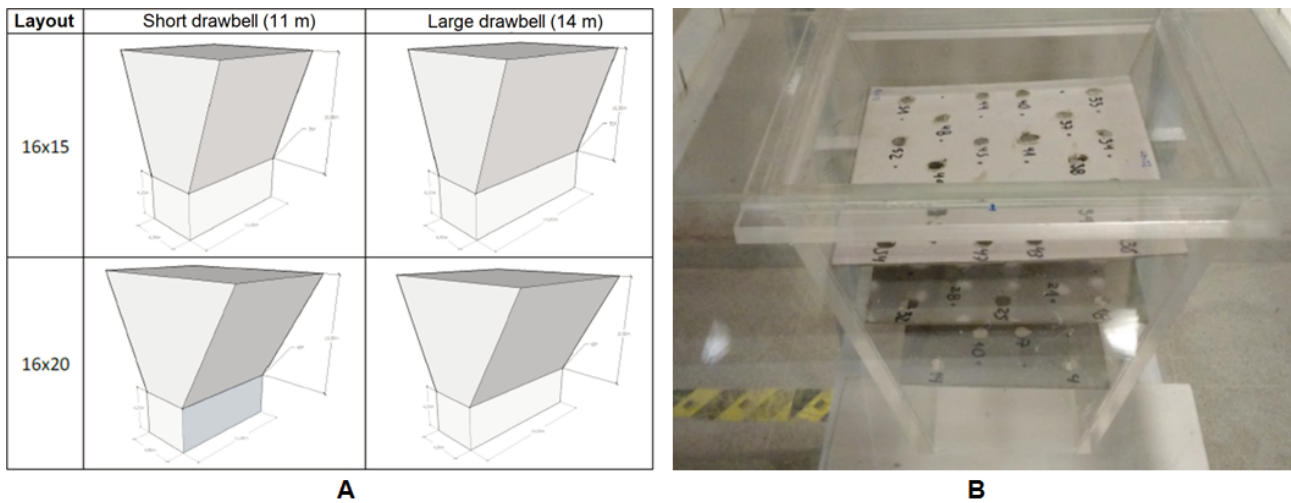


**Figure 4 (a) Various drawbell geometries tested in gravity flow experiments; (b) Example of marker locations inside the drawbell**

Markers also are located inside the drawbell (Figure 4b) to analyse the evolution of the extraction zone during the extraction from both drawpoints. Different drawbell configurations have been used to study the drawbell’s geometry on the extraction zone, the movement zone, the productivity and the hang-up frequency (Castro et al. 2020a).

In terms of fine material migration, various experimental setups have been tested, such as stope geometry, high draw column, isolated and interactive draw strategies, influence of non-draw zone, and different particle size distributions of coarse material (Armijo et al. 2014; Castro & Pineda 2015; Castro et al. 2022a; Olivares et al. 2015; Vergara 2016). However, the main parameter in these studies is the ratio between the fine material and the coarse material tested, and how this impacts on the dilution entry (Laubscher 1994, 2000b; Hashim et al. 2008). Figure 5 shows an example of the relation between the fine and coarse materials tested in a gravity flow study of fine migration (Castro et al. 2022a).

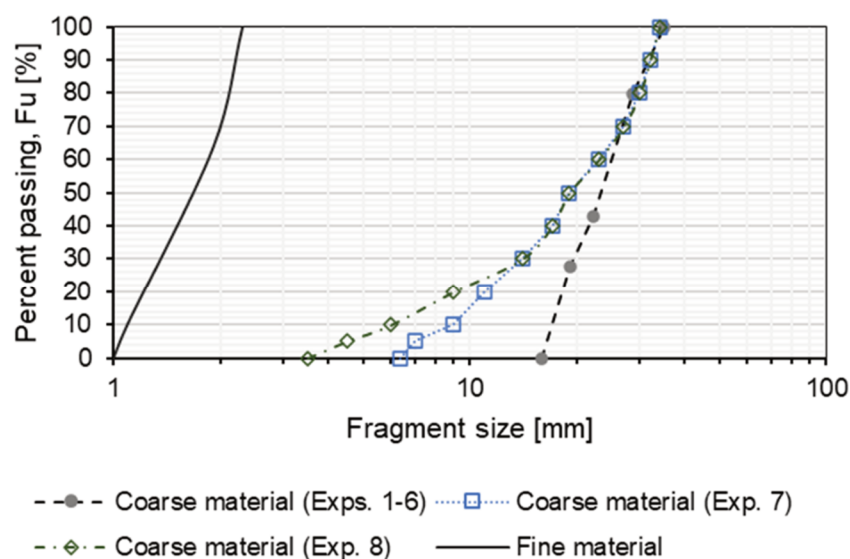


**Figure 5 Particle size distribution curve used in studies of fine material migration (Castro et al. 2022a)**

On the other hand, the stresses in experiments of gravity flow are studied using load sensors located in the wall of the models or over the pillars to measure horizontal and vertical stresses. The load sensors located on the model walls (Figure 6a) measure horizontal stresses in the broken column. The load sensors placed inside the model (Figure 6b) allow stresses in the flow zones to be measured.

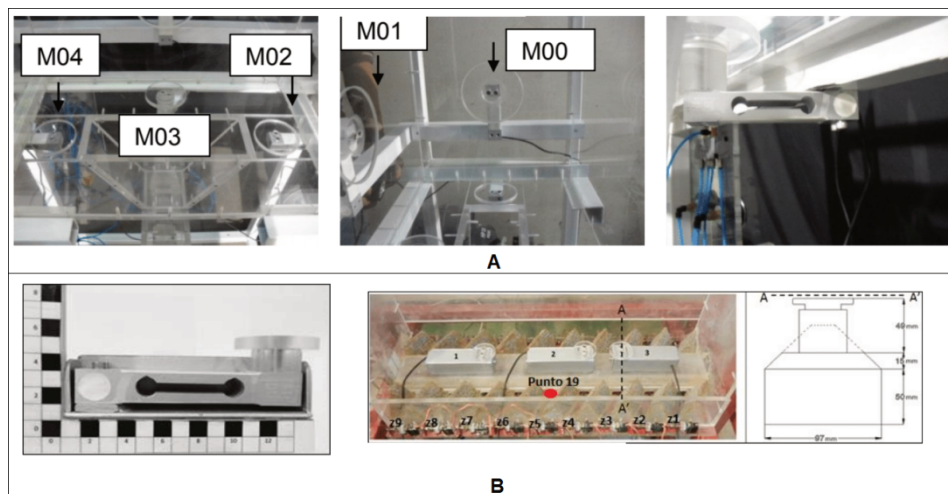


**Figure 6** Load sensors used in gravity flow experiments. (a) Examples of load sensors located on the model walls for vertical and horizontal stress measurement; (b) Examples of load sensors located inside the model for vertical stress measurement

Granular material fragmentation has also been quantified in gravity flow experiments. These experiments used a press machine to apply high pressures on the material (Figure 1b). These high pressures are required because the material tested has high strengths (uniaxial compressive strength between 30–160 MPa). Pressures applied with the press machine on the granular material are between 0–6 MPa. These pressures break the rock fragments during flow experiments. The degree of fragmentation is quantified through sieving of the initial and final fragment size distribution of the materials. Nevertheless, the fragmentation has also been quantified under low stresses to measure the effect of the travel distance on granular material fragmentation (Gómez & Castro 2022a).

The productivity and hang-ups events are quantified during the flow experiments. Mass-per-extraction cycle (with LHD or dozer systems) is quantified and then scaled to determine the productivity of the experimental setups tested. In some experiments, hang-ups formed by coarse arches appear due to coarse fragmentation or high pressures. Figure 7 shows an example of a coarse hang-up under low stress over the drawpoint.



**Figure 7** Hang-up formed by a coarse arch of random rock fragment

Finally, some experiments have been developed using different amounts of fine material and water content (Castro et al. 2022c; Olivares 2015; Sánchez et al. 2019). These setups have been done to study the flowability

of the granular material, the geometry of flow zones, hang-ups formed by cohesive arches, and extraction equipment capability.

### 3 Experiments in gravity flow

In this section a summary of the main significances of the experimental result carried out to date in the Block Caving Laboratory is presented.

#### 3.1 Flow geometry

The geometry of the movement and extraction zones are commonly quantified in the experiments through the markers described in Section 2.3. Several results have been observed here such as the effect of fragment size, undercutting height, and moisture on the width of the flow zone. Small flow widths are expected by fine particle size distribution (PSD) as the literature indicates.

The results confirmed that moisture content affects the geometry of flow zones, the experimental data indicated that the diameter increased with a different rate of growth depending on moisture content (Sánchez et al. 2019). The diameter of the drawzones tended to stabilise over time with wet samples, while the draw zone diameter with dry samples (0–2% moisture content) continued to increase with the mass drawn. The geometry of the flow zone was characterised in terms of its height and width (Figure 8). Figure 8a shows that the height of extraction increases with mass for all tests where moisture content was below 6%.

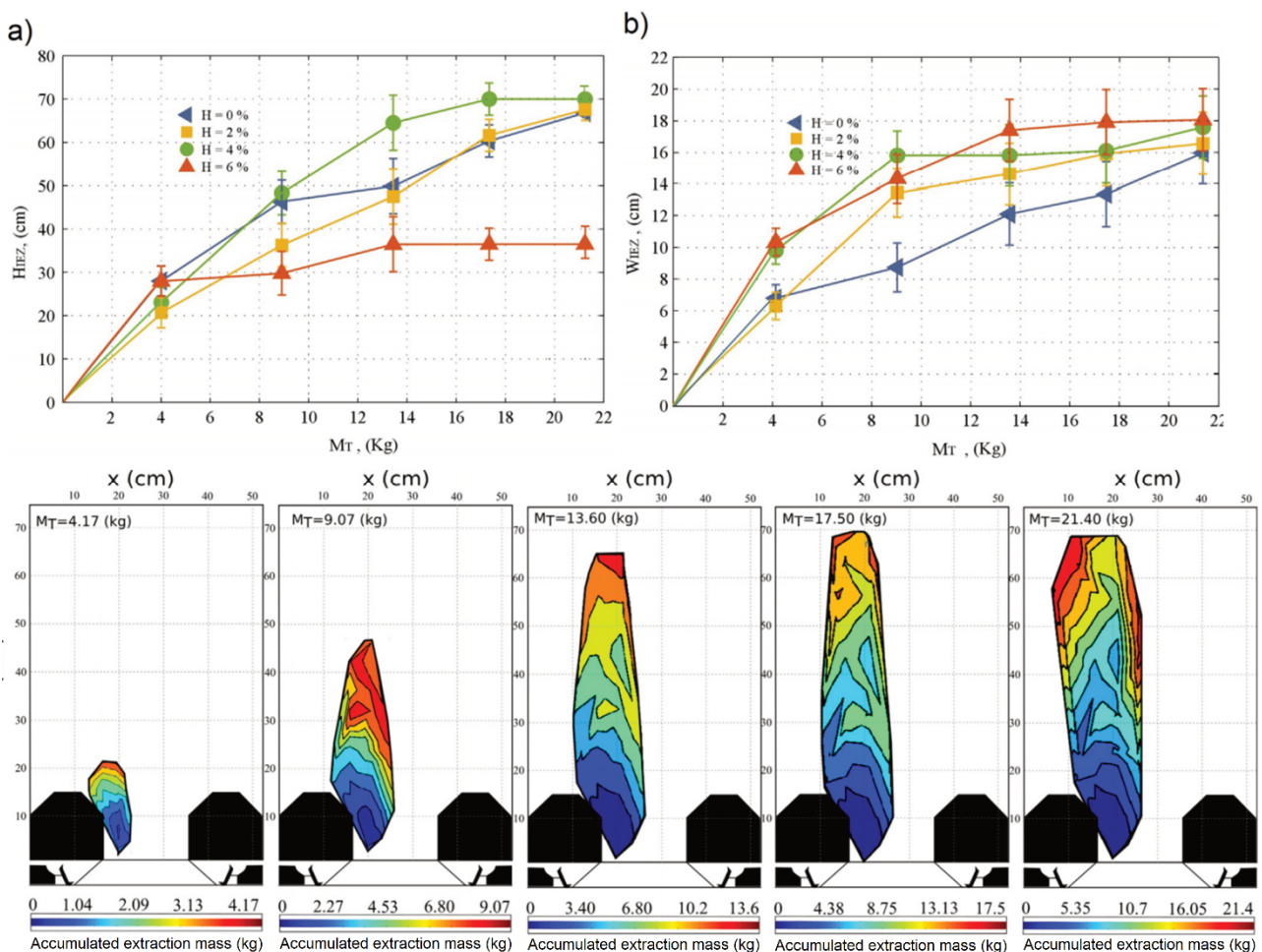


**Figure 8** (a) Isolated extraction zone height as function of the mass draw for different moisture contents; (b) Isolated extraction zone width as function of the mass draw for different moisture contents; (c) Example of the evolution of flow experiment for 4% of moisture

Figure 8c shows the evolution of the flow zone during the experiments for isolated draw. In these experiments the dimensionless flow width number ( $W_{FZ}/D_W$ ; width of flow zone and drawpoint width) indicates that the flow zones are within the range of 2.7 to 3 times the drawpoint width, which is within the range of expected results in the literature. In Figure 9, a model with one drawbell scaled 1:50 is used to study the effect of the undercutting height (represented with finer granular material) on gravity flow.

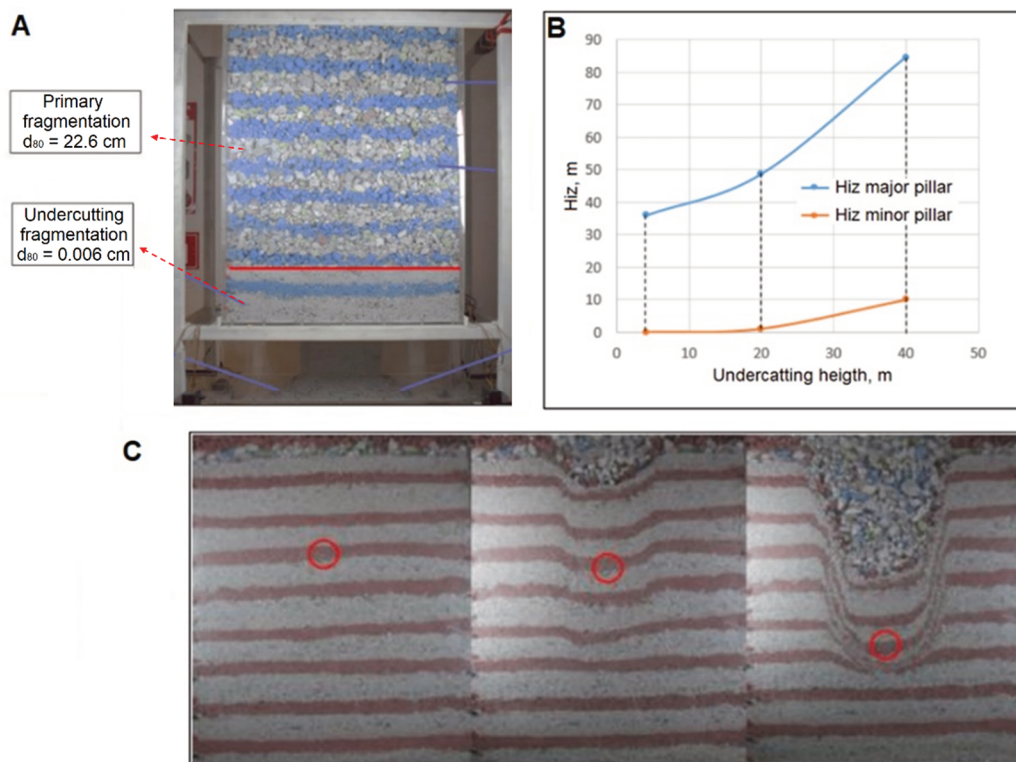


**Figure 9 (a) Experimental setup to study the effect of the undercutting height, scale 1:50; (b) Height of the interaction scaled from experimental results; (c) Experiment evolution during draw**

The height of the interaction zone (Figure 9b) was determined over the major and minor pillars. In the experiments, undercutting heights from 4–40 m were evaluated. We observed that the finer material increases the height of the interaction zone especially over the major pillar (crown pillar).

On the other hand, a large physical model was built to simulate a large draw area in a panel caving draw strategy. The model is 2.5 m × 1.6 m × 0.23 m (height × width × depth) with 48 drawpoints and represents a broken column height of 500 m (scaled 1:200). In this model, the extraction drift (Z44) is not drawn and was studied if the neighbouring extraction drifts interact. Figure 10 shows when the interaction is reached in the model at 80 m of height after drawing 36% of the drawn column. Then, the height of interaction decreased to 50 m due to draw.



**Figure 10 Experiment evolution in large physical model during draw in a panel caving draw strategy (Vergara 2016)**

### 3.2 Migration of fine material

Fine material migration in caving mines is a critical parameter that must be controlled during ore extraction. This is because decreasing ore grade could imply ore losses. Moreover, the fine material could generate inrush of fine event or mud rush events if mixed with water. Thus, the dilution entry must be avoided or postponed to decrease its consequences.

Various experimental setups have been developed to study the main variables of fine material percolation (Armijo 2014; Castro & Pineda 2015; Castro et al. 2022a; Vergara 2016). In these experiments variables such as large-stope geometry, draw strategies, ratio between coarse and fine material, height of coarse and fine material, and fragment size distribution have been studied. Figure 11 shows dilution entry in a large inclined stope where material was drawn from 11 drawpoints at the bottom.

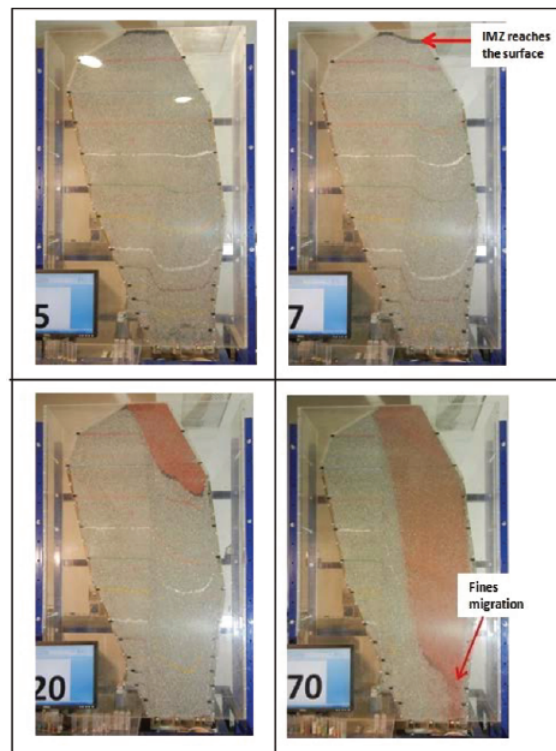


**Figure 11 Large-stope model, scaled 1:50, used to study the ore recovery before dilution entry (Castro & Pineda 2015)**

In Armijo et al. (2014), the effect of isolated and uniform draw is tested in a high draw column (draw column height of 500 m real-scale, 2.5 m at laboratory-scale). The ratio between mean size ( $d_{50}$ ) was 31.8, with a coarse mean fragment of 4.45 mm and a fine mean fragment of 0.14 mm. Figure 12 shows the experiments carried out. In the isolated draw (Figure 12 top), the fine material entry in drawpoint is 60% of total mass. In the uniform draw, the fine material entry in drawpoint is 95% of total mass. In this last experiment, the shear strain does not occur, decreasing the percolation of fine material.



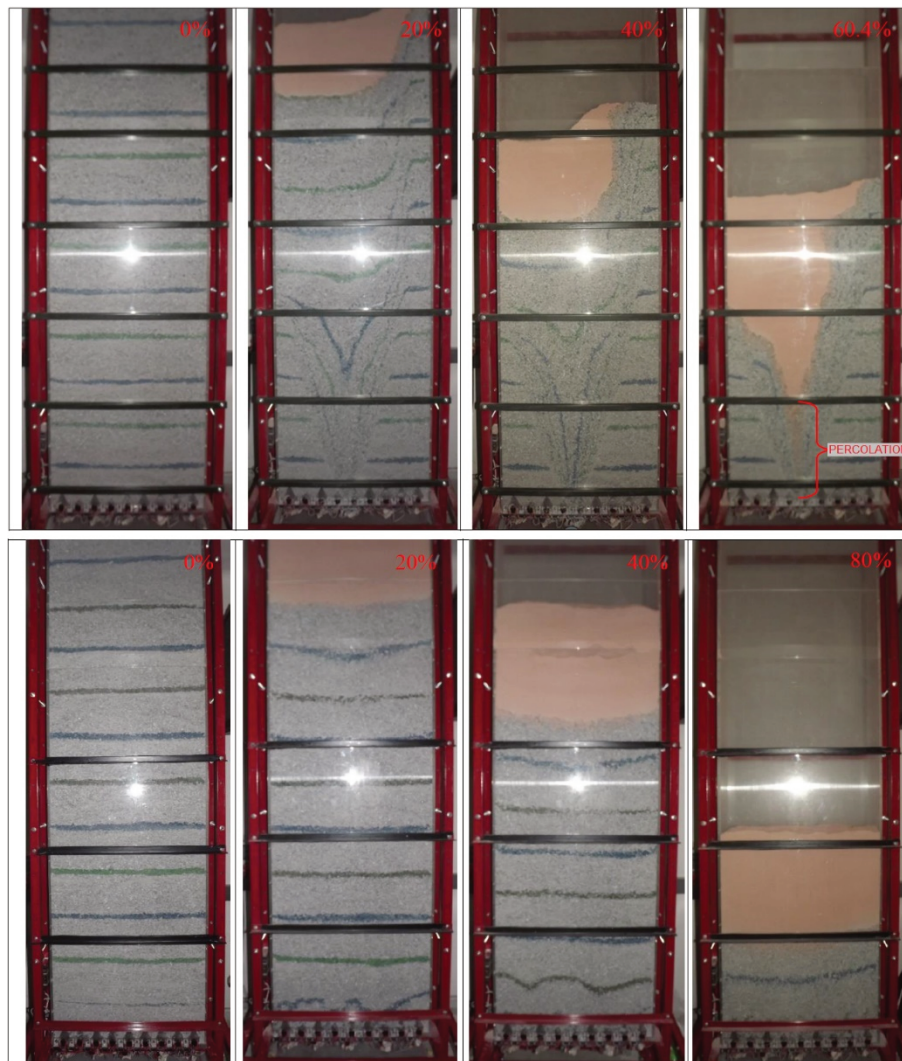


**Figure 12 High draw column migration study (Armijo et al. 2014)**

A physical model with one drawbell, scaled 1:50, was used to study the influence of key variables reported in theory (Bridgwater et al. 2003; Cooke et al. 1978; Hashim 2011; Laubscher 2000b) on fine material migration. In this model different ratios between coarse and fine materials, different coarse material distribution, and different materials' heights were tested. This physical model (Figure 13) replicates a drawbell with two drawpoints where material was drawn by two LHD scaled units. A total of eight experimental setups were developed, in which dilution entry was reported in all of them due to particle percolation during draw (Castro et al. 2022a).



**Figure 13 Fine migration test evolution during draw in a physical model scaled 1:50 (Castro et al. 2022a)**

The experimental results are presented in Figure 14, the ratio between mean fragment of coarse and fine material ( $d_{50}$ ) and the coefficient of uniformity ( $C_u = d_{60}/d_{10}$ ) are indicated. Results confirm that under one drawpoint extraction the dilution entry was anticipated. Also, for higher height of fine material over the draw column the fine material migration increased. The fragment size distribution of the coarse material also influences the dilution entry; wider distributions show lower migration because there are less voids between fragments. These experiments allow a migration logic in a gravity flow simulator to be implemented and calibrated (Castro et al. 2022b).

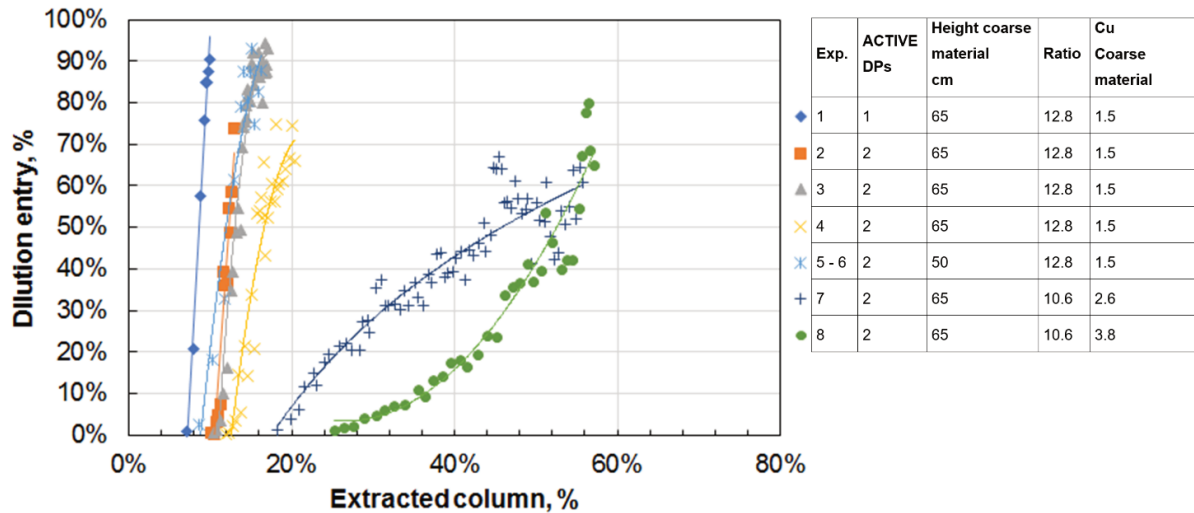


**Figure 14 Dilution entry observed in the fine migration experiment for caved material (Castro et al. 2022a).  $H_c$  is the height of broken column (coarse material),  $H_f$  is the height of fine material, and FSD is the fragment size distribution of coarse material used (wider for test 7 and 8)**

### 3.3 Stresses measurement under draw

Usually in block caving mines, when the caving propagation connects to surface, vertical stresses over the production drift is not closely monitored. However, experience indicates that production drift stability can also be affected during ore extraction in the production level (Orellana et al. 2014; Pierce 2019; Sahupala et al. 2008). Here, stresses have been measured in two different physical models. A model has a drawbell scaled 1:50 and built with 36 drawpoints scaled 1:200 (Castro et al. 2020b; Orellana 2012).

The first physical model was filled with gravel material and used dozer extraction equipment below the drawbell (Orellana 2012). In this experimental setup, vertical stresses were measured over the pillar and horizontal stresses on the model wall (Figure 6a). The vertical stresses measured in static condition had direct correlation with the materials' density, observing the Janssen effect (Sperl 2006) due to arching. As expected, stress distribution was observed during draw, when extraction initiated initial stress (horizontal and vertical) changes until reach a regimen state in dynamic condition (Figure 15).

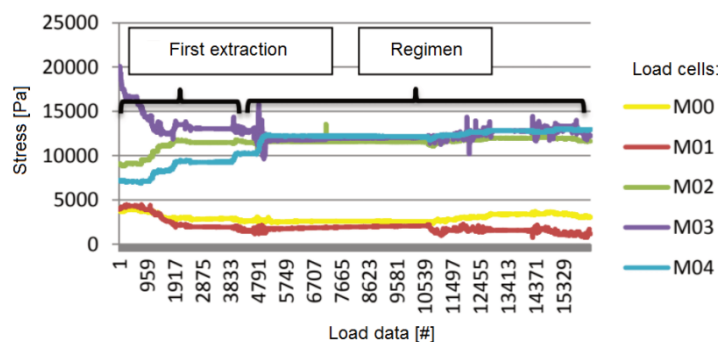


**Figure 15 Stress results measured in experiment during draw from a drawbell with dozer extraction equipment (scale 1:50) (Orellana 2012)**

The result obtained in the physical model showed the high variability of stresses during draw, but the model cannot predict what would occur in a large layout for different draw strategies. Thus, a model scaled 1:200 was built and filled with ore material in a block caving layout with 36 drawpoints (Castro et al. 2020b). In this model the effect of the draw strategy on the induced vertical stresses in the granular material was studied. Here, three draw strategies were studied: isolated draw, panel caving draw, and block caving draw. Vertical stresses ( $\sigma_v$ ) were measured in the movement and stagnant zones where variations are between 0.3 and 2.8 times their initial value ( $\sigma_{v,0}$ ). The stresses induced are highly influenced by both the distance from the extraction front and the dimension of draw and non-draw areas. Figure 16 shows a summary of the vertical stress observed in the panel and block caving draw strategies for different ratios between the stagnant area ( $A_{SZ}$ ) and the total area ( $A_T$ ).

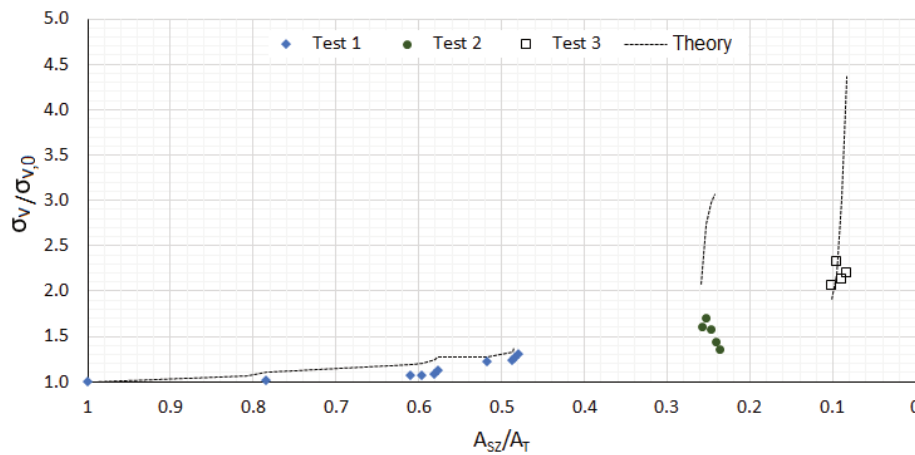


**Figure 16 Vertical stress ( $\sigma_v$ ) normalises by its initial value ( $\sigma_{v,0}$ ). Results measured in the experiment during draw in panel caving strategy (Test 1) and block caving strategies (Test 2 and 3) (Castro et al. 2020b)**

The initial vertical stresses were calculated using the Janssen approach (Sperl 2006):

$$\overline{\sigma_{v,0}} = \frac{R_h \rho_b g}{\mu k} \left( 1 - e^{-\frac{\mu k z}{R_h}} \right) + Q_0 \left( e^{-\frac{\mu k z}{R_h}} \right) \quad (1)$$

Where  $R_h$  is the hydraulic radius (area/perimeter; m) introduced by (Jenike et al. 1973),  $\rho_b$  is the bulk density ( $\text{kg/m}^3$ ),  $g$  is the gravity constant ( $\text{m/s}^2$ ),  $k$  is the friction parameter that represents the horizontal and vertical stress ratio,  $\sigma_h/\sigma_v$ ,  $z$  is the depth of caved rock (m),  $Q_0$  is the initial vertical overload (Pa), and  $\mu$  is the friction between particles and model wall expressed usually by  $\tan(\phi_w)$ , where  $\phi_w$  is the friction angle of bin walls (degrees). This equation gives a reasonable result in static conditions. While the vertical stress in the stagnant zone,  $\sigma_v^{SZ}$  is calculated by rewriting the equation proposed by Pierce (2009) and normalising it by the initial vertical stress,  $\sigma_{v0}$  as:

$$\frac{\sigma_v^{SZ}}{\sigma_{v0}} = \left( A_T - \frac{\sum \sigma_v^{MZ} A_{MZ}}{\sigma_{v0}} \right) \frac{1}{A_{SZ}} \quad (2)$$

Where  $\sigma_{v0}$  is the initial vertical stress,  $A_T$  is the total caved area,  $\sigma_v^{MZ}$  is the vertical stress in the movement zone,  $A_{MZ}$  is the area of the movement zone, and  $A_{SZ}$  is the area of the stagnant zone.

### 3.4 Hang-up events

Coarse arches are a common issue in caving mines where large fragments are expected. These arches interrupt ore flow in drawpoints, decreasing available draw area, and increasing the possibility of non-uniform draw, which can increase fine migration, mud rush risk, and induced stress in the caved column. Hang-ups due to coarse arching has been studied in various physical models (Castro et al. 2016; Castro et al. 2020a; Castro et al. 2014; Orellana 2012), where the main variable measured has been the hang-up frequency (g/hang-up), and additionally, the hang-up index in mine scale (# hang-ups/1,000 t) and the height of

hang-ups have been quantified. Orellana (2012) tested different granular materials where it was concluded that fragment strength and sphericity decreased hang-up events. The effect of vertical load on gravity flow tests (from 0–6 MPa, using a press machine) allowed different flow conditions to be identified (Figure 17a), as well as quantifying the effect of vertical load on the hang-up frequency (Figure 17B).

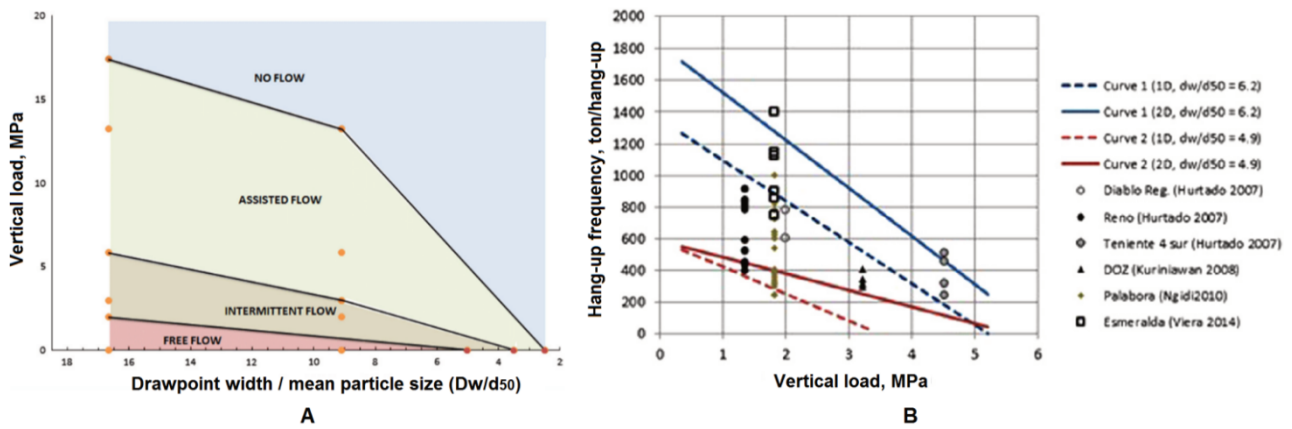


**Figure 17 (a) Flow conditions under confinement and the ratio between the drawpoint width and the mean fragment size (Castro et al. 2014); (b) Hang-up frequency under confinement condition and mine data (Castro et al. 2016)**

The ratio between the drawpoint width and the fragment size, as well as the pressures in the granular material, had highly influenced hang-up events. Moreover, other parameters have influence too, such as the drawbell geometry. Thus, experiments have been developed for different drawbell geometries (Figure 4a) to study the hang-up formation (Castro et al. 2020a). In these experiments, the drawbell length and width at the bottom show high influence on hang-up formation. These results can be presented in term of volumes (Figure 18).

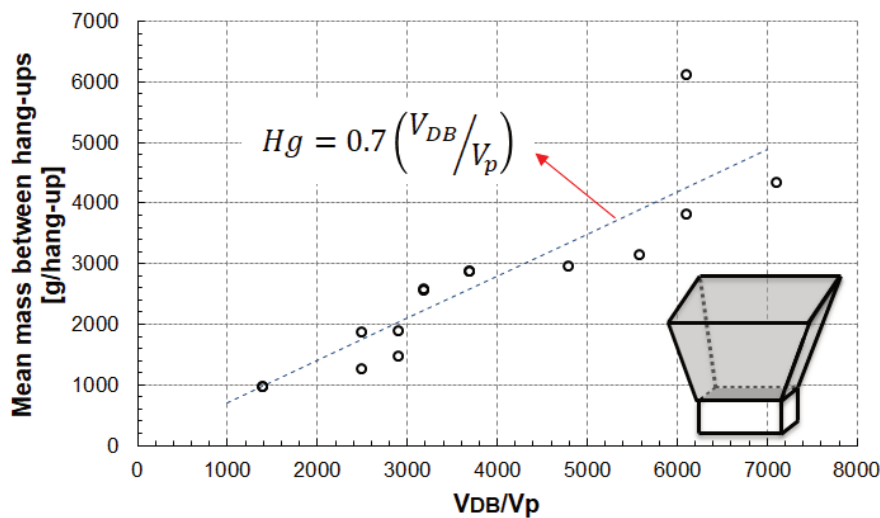


**Figure 18 Drawbell volume ( $V_{DB}$ ) and particle volume ( $V_p$ ) effect on hang-up frequency. Model scale 1:50 (Castro et al. 2020a)**

The drawbell volume increases the mass between hang-ups. This relation can be approximated linearly, as shown by  $H_g$  (mean mass between hang-ups) for the experimental results. The hang-up described above is related to coarse arches. However, cohesive arches also have been studied during gravity flow experiments (Olivares et al. 2015; Sánchez et al. 2019). The formation of cohesive arches generated at laboratory-scale by the combinations of moisture content and fine material variables did provide information about the mechanisms involved. In Figure 19, examples of hang-ups due to cohesive materials are observed.

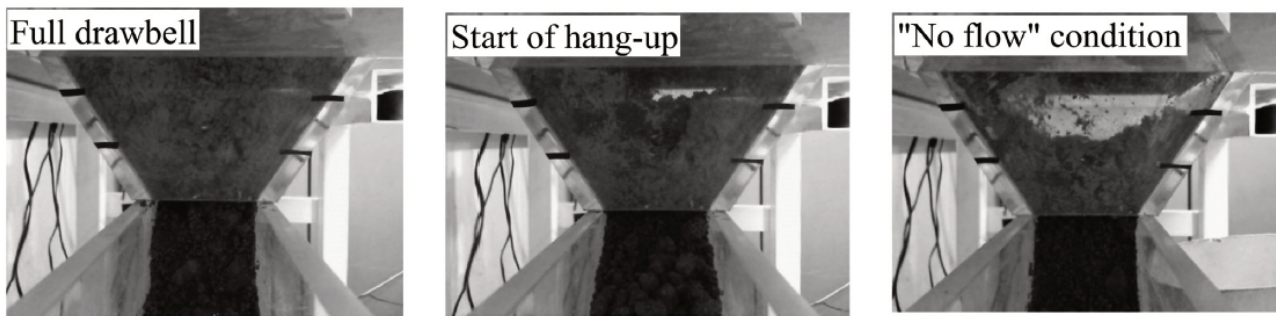


**Figure 19 Evolution of a non-flow condition due to a cohesive hang-up (model scale 1:75) (Sánchez et al. 2019)**

Through the study presented in Figure 19, it was also possible to identify that the diameter of the drawzones is 2.7–3 times the drawpoint width for fine fragmented rock in comparison to what is being used for design guidelines; for this reason, in modern LHD drawpoint spacing, ore recovery is expected to be low. The mass drawn between hang-ups shows a dependency on moisture content and number of drawpoints. The higher the moisture content, the less mass can be drawn between events. Drawing from two drawpoints allows for drawing more between events than when drawing in isolated conditions.

### 3.5 Fragmentation due to draw and overload

Ore fragmentation has been highly studied based on different rock properties, load conditions, dry and wet environments and draw rates (Castro 2016; Gómez et al. 2017, 2021; Gómez & Castro 2022a; Torres 2019). These studies were developed mainly to analyse the secondary fragmentation within the draw column. Moreover, a secondary fragmentation model, the Block Caving Comminution Model (BCCM) (Gómez et al. 2017, 2021), has been developed through experimental data and has been compared with fragment size distribution from a Chilean copper mine giving reasonable approach.

The experimental setup used considers the confined model (Figure 1b) and the various granular materials. Here, the rock fragmentation occurs in draw-confined tests (0–6 MPa) due to abrasion and compression mechanisms. Fragmentation by compression occurs despite the strength of fragment tested because the stress concentration in the contact points between fragments overcomes the point load index of rock. The effect of load on fragmentation can be noticed in Figure 20a, while fragmentation by abrasion is related mainly due to ore draw. This can be observed in test under confinement without draw and with draw in Figure 20b (Gómez et al. 2017), and in the tests of different travel distances under low load (Figure 20c) (Gómez & Castro 2022a).

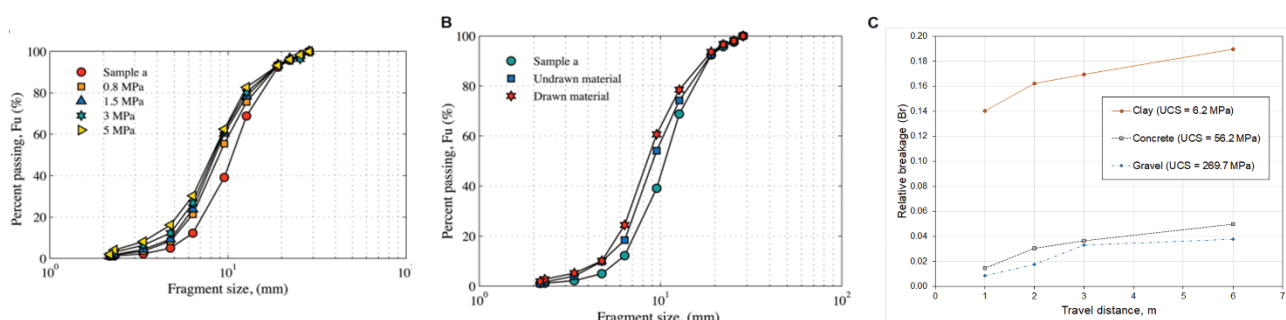


**Figure 20 Fragmentation tests. (a) Influence of load; (b) Draw and no draw tests; (c) Effect of travel distance under low load**

### 3.6 Mud extraction

Experiment of mud extraction is one of the most recent experimental setups developed in the Block Caving Laboratory. The experiment was developed to understand the critical condition that an LHD without an operator could work in a drawpoint with a high percentage of moisture and fine materials. Nowadays, the drawpoints are closed if it has a critical moisture level and fine materials amount to prevent a mud rush event.

In the tests, material from a Chilean copper mine with mud rush problems was used. First, the material was characterised with the Abrams cone (ASTM International 2003) to determine the moisture percentage that the material had a plastic and fluid behaviour. The use of the Abrams cone to characterise material for mud rush purposes was introduced by Vallejos et al. (2017). Figure 21 shows the Abrams cone test for the material used in experiments as well as the number of mud events for the moisture percent used.

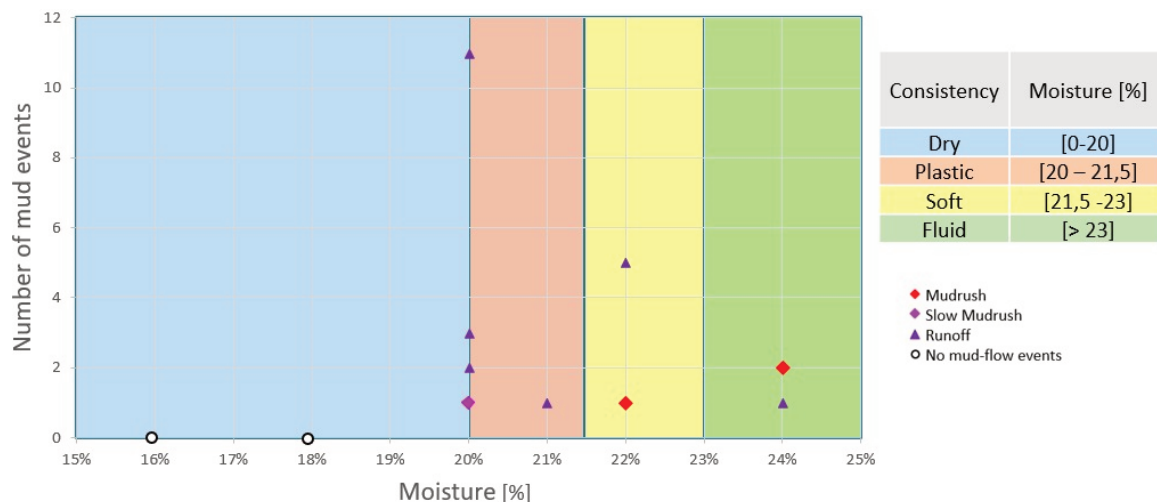


**Figure 21 Abrams cone characterisation and mud events reported in flow experiments (Castro et al. 2022c)**

The material consistency used to characterise the extracted material was also useful at laboratory scale. The magnitude of the mud-flow event was observed to increase with more fluid material consistencies. On the other hand, cohesive hang-ups induced by water in fines, increased the risk of mud-flow events because mud material can be retained close to the drawpoint (Castro et al. 2022c). Although cohesive hang-ups have been reported at low moisture percentages (Sánchez et al. 2019). and they have been observed to increase with the presence of water (Castro et al. 2016) until soft and fluid consistencies are reached as we observed in our experiments.

The PSD is key in mud-flow events. In this study, coarse fragments in the PSD were usually observed in the hang-ups prior to a mud-flow event. However, there are some questions that still must be studied, such as the relation between the PSD and cohesive hang-ups, the amount of mud material that could be retained by the PSD in cohesive hang-ups, and the relationship between PSD in mud-flow events and the magnitude of event.

## 4 Physical experiments as a tool for numerical model calibration

The physical experiments are also used to calibrate numerical models. For example, some of the experiments described in Section 3 have been used to calibrate a flow simulator based on cellular automata (Castro et al. 2022b; Gómez & Castro 2022b). In Castro et al. (2022b), the experiments of fine material migration presented in Section 3.2 were used to calibrate a migration logic implemented in the numerical flow simulator. In Gómez & Castro (2022b), the stress experiments presented in Section 3.3 were used to calibrate the stress model also applied in the gravity flow simulator as is shown in Figure 22.

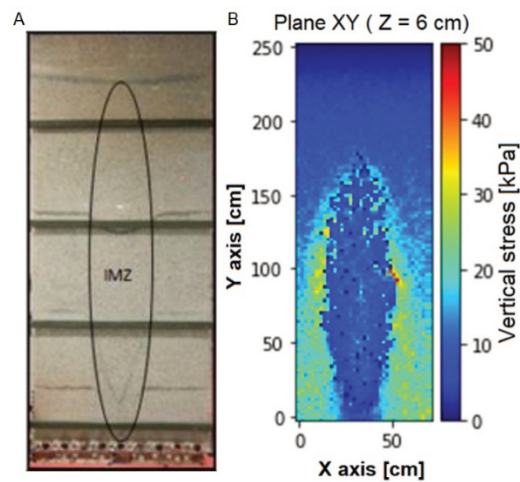


**Figure 22 (a) Stress measurement experiment under isolate draw; (b) Stress model based on cellular automata under isolated draw**

Also, some physical experiments (Castro et al. 2016; Castro et al. 2020a; Gómez et al. 2017) (Figure 23a) have been used to calibrate DEM simulations using Esys-Particle software. In Figure 23b the effect of the vertical pressure on hang-up events (Cid 2019) was numerically studied. In Figure 23c the fragmentation mechanisms that occur during gravity flow under confinement (Jimenez 2020) was studied. These numerical simulations were successfully calibrated with physical experiments.

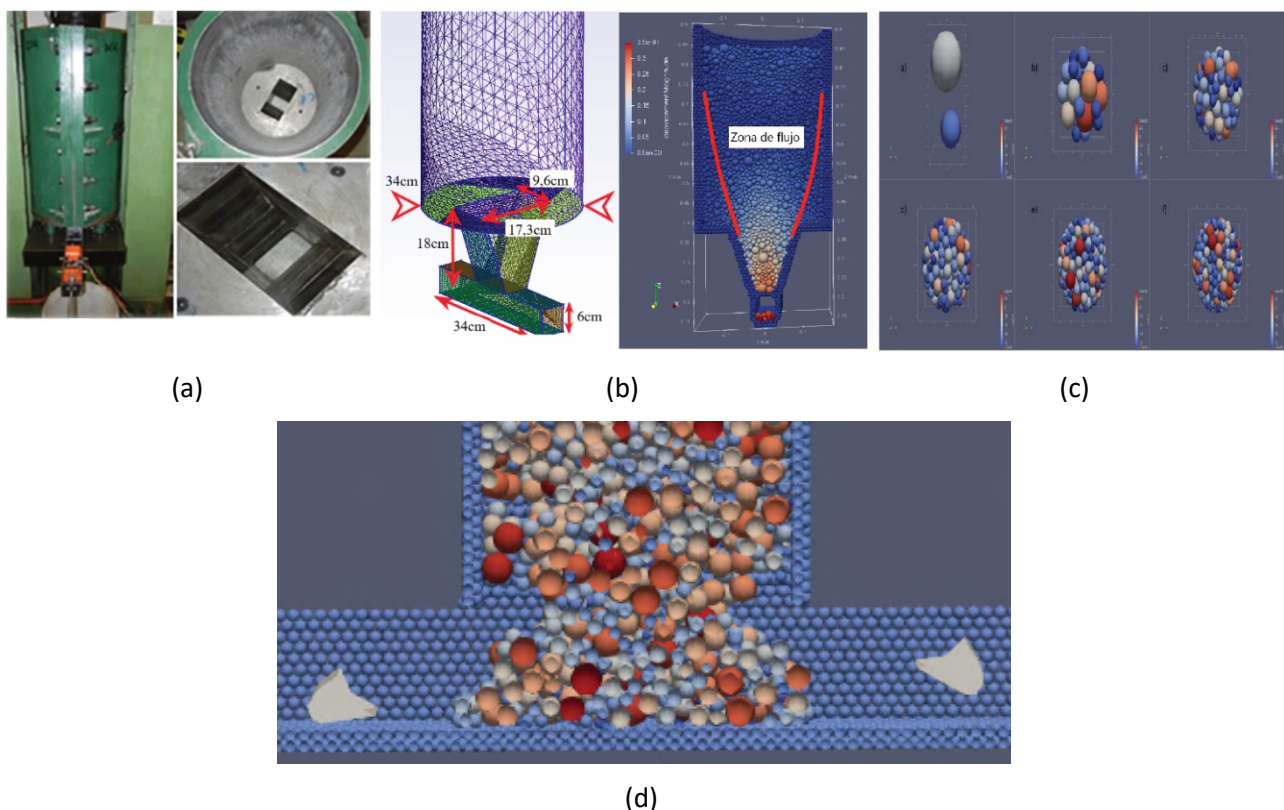


**Figure 23 (a) Confined flow physical model; (b) DEM simulation used to study hang-up events; (c) DEM simulation used to study particle fragmentation during flow; (d) DEM simulation used to study the drawbell geometry**

In drawbell geometry studies, physical experiments (Castro et al. 2020a) have been used to calibrate numerical models and evaluate different geometries. During calibration, the tonnage between hang-ups was compared between the physical and the numerical model, with an absolute error of 9%. Then, the drawbell

performance was analysed comparing the geometries shown in Figure 24. The preliminary outcomes are shown in the Table 1. The El Teniente drawbell presents a hang-up frequency 13% higher than the base case. The circular drawbell has smaller drawbell volume than the other drawbells.

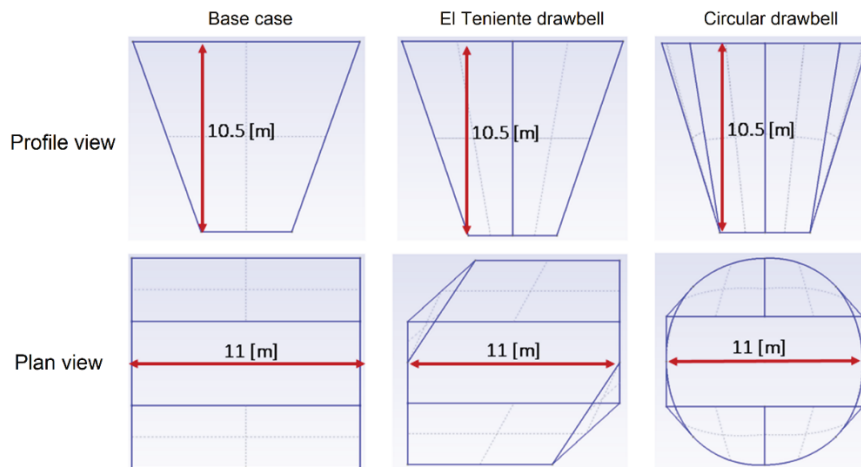


**Figure 24 Geometries of drawbell analysed in the numerical model**

**Table 1 Performance of drawbell in the numerical model**

Drawbell	Tonnage between hang-ups (tonnes)	Relative performance	Hang-ups/1,000 tonnes	Drawbell volume (m <sup>3</sup> )
Base case	110 ± 118	–	9.1	1,670
Circular	128 ± 97	16%	7.8	1,360
El Teniente	96 ± 86	-13%	10.4	1,510

## 5 Conclusion

The experimental results presented in this paper show that several variables can be studied in laboratory condition representing scaled mine design, that are usually difficult to study at the mine scale. In experiments using physical models, we can observe and quantify variables of interest. However, scaling limitations should be known in this study to understand the scopes of the results obtained. However, the physical models are important tools to generate new knowledge about planning and mine design. Additionally, physical models give important data for calibrating numerical models. In terms of block caving studies, the representation of the geometry, material and extraction system gives us good geometrical similitude in the scale models. These experiments are a mine engineering tool that allow various caving phenomena related to gravity flow to be analysed.

## Acknowledgement

This paper was funded by the CONICYT/PIA Project AFB180004.

## References

- Armijo, F, Irribarra, S & Castro, R 2014, 'Experimental study of fines migration for caving mines', in R Castro (ed), *Caving 2014: Proceedings of the 3rd International Symposium on Block and Sublevel Caving*, Universidad de Chile, Santiago, pp. 356–362.
- ASTM International 2003, *Standard Test Method for Slump of Hydraulic-Cement Concrete (ASTM C143 2003)*, ASTM International, West Conshohocken.
- ASTM International 2002, *Standard Test Methods for Absorption and Bulk Specific Gravity of Dimension Stone (ASTM C97 2002)*, ASTM International, West Conshohocken.
- ASTM International 2018, *Standard Test Methods for of Soil Specific Gravity Solids by Water Pycnometer (ASTM D 854 2018)*, ASTM International, West Conshohocken.



- ASTM International 2011, *Standard Test Method for Direct Shear Test of Soils under Consolidated Drained Conditions (ASTM D3080/D3080M 2011)*, ASTM International, West Conshohocken.
- ASTM International 2008, *Standard Test Method for Determination of the Point Load Strength Index of Rock and Application to Rock Strength Classifications (ASTM D5731 2008)*, ASTM International, West Conshohocken.
- Baxter, GW 2012, 'Cellular automata models of granular flow', *Experimental and Computational Techniques in Soft Condensed Matter Physics*, 9780521115(2), pp. 209–229.
- Bock, S & Prusek, S 2015, 'Numerical study of pressure on dams in a backfilled mining shaft based on PFC3D code', *Computers and Geotechnics*, vol. 66, pp. 230–244.
- Bridgwater, J, Utsumi, R, Zhang, Z & Tuladhar, T 2003, 'Particle attrition due to shearing - the effects of stress, strain and particle shape', *Chemical Engineering Science*, vol. 58, no. 20, pp. 4649–4665.
- Brown, ET 2007, *Block Caving Geomechanics*, 2nd edn, Julius Kruttschnitt Mineral Research Centre, The University of Queensland, Brisbane.
- Brunton, I, Lett, G & Sharrock, G 2016, 'Full-scale flow markers experiments at Ridgeway Deeps and Cadia East Cave Operations', *MassMin 2016: Proceedings of the Seventh International Conference & Exhibition on Mass Mining*, Australasian Institute of Mining and Metallurgy, Melbourne, pp. 817–824.
- Calderon, C, Alfaro, M & Saavedra, J 2004, 'Computational model for simulation and visualization of gravitational flow', in A Karzulovic & M Alfaro (eds), *Proceedings of Massmin 2004*, Instituto de Ingenieros de Chile, Santiago, 185–188.
- Castro, R, Gómez, R & Hekmat, A 2016, 'Experimental quantification of hang-up for block caving applications', *International Journal of Rock Mechanics and Mining Sciences*, vol. 85, pp. 1–9, <http://dx.doi.org/10.1016/j.ijrmmms.2016.02.005>
- Castro, RL, Basaure, K, Palma, S & Vallejos, J 2017, 'Geotechnical characterization of ore related to mudrushes in block caving mining', *Journal of the Southern African Institute of Mining and Metallurgy*, vol. 117, no. 3, pp. 275–284.
- Castro, R & Pineda, M 2015, 'The role of gravity flow in the design and planning of large sublevel stopes', *Journal of the Southern African Institute of Mining and Metallurgy*, vol. 115, no. 2, pp. 113–118.
- Castro, R 2007, *Study of the Mechanisms of Gravity Flow for Block Caving*, The University of Queensland, Brisbane.
- Castro, R, López, S, Gomez, R, Ortiz, S & Carreño, N 2020a, 'Experimental study of the influence of drawbell geometry on hang-Ups in cave mine applications', *Rock Mechanics and Rock Engineering*, vol. 54, no. 1, pp. 1–10.
- Castro, R, Gómez, R, Pierce, M & Canales, J 2020b, 'Experimental quantification of vertical stresses during gravity flow in block caving', *International Journal of Rock Mechanics and Mining Sciences*, vol. 127.
- Castro, R, Arancibia, L & Gómez, R 2022a, 'Quantifying fines migration in block caving through 3D experiments', *International Journal of Rock Mechanics and Mining Sciences*, vol. 151, pp. 8–10.
- Castro, R, Gómez, R & Arancibia, L 2022b, 'Fine material migration modelled by cellular automata', *Granular Matter*, vol. 24, no. 1, pp. 1–11.
- Castro, R, Betancourt F, Gómez R, Salas, O & Zarabia, J 2022c, 'Experimental study of mudrush mechanisms in block caving', *Mining, Reclamation and Environment*, under review.
- Castro, RL, Fuenzalida, MA & Lund, F 2014, 'Experimental study of gravity flow under confined conditions', *International Journal of Rock Mechanics and Mining Sciences*, vol. 67, pp. 164–169.
- Cho, Gye-Chun, Dodds, J & Santamarina, JC 2006, 'Particle shape effects on packing density, stiffness, and strength: natural and crushed sands', *Journal of Geotechnical and Geoenvironmental Engineering*, vol. 132, no. 5, pp. 591–602.
- Cid, P 2019, *Simulación de Flujo Gravitacional En Batea de Extracción a Través de Elementos Discretos*, Universidad de Concepción, Concepción.
- Cleary, PW & Sawley, ML 2002, 'DEM modelling of industrial granular flows: 3D case studies and the effect of particle shape on hopper discharge', *Applied Mathematical Modelling*, vol. 26, no. 2, pp. 89–111.
- Cooke, MH, Bridgwater, J & Scott, AM 1978, 'Interparticle percolation: lateral and axial diffusion coefficients', *Powder Technology*, vol. 21, no. 2, pp. 183–193.
- Dassault Systèmes 2018, *PCBC*, computer software, <https://www.3ds.com/products-services/geovia/products/pcbc/>
- ESSS 2022, *Rocky DEM*, computer software, <https://rocky.esss.co/new/new-rocky-dem-2022r1/>
- Gómez, R, Castro, R, Casali, A, Palma, S & Hekmat, A 2017, 'A comminution model for secondary fragmentation assessment for block caving', *Rock Mechanics and Rock Engineering*, vol. 50, no. 11, pp. 3073–3084.
- Gómez, R, Castro, R, Betancourt, F & Moncada, M 2021, 'Comparison of normalized and non-normalized block caving comminution models', *Journal of the Southern African Institute of Mining and Metallurgy*, vol. 121, no. 11, pp. 581–588.
- Gómez, R & Castro, R 2022a, 'Experimental quantification of granular material fragmentation due to travel distance', *Mining, Metallurgy & Exploration*, vol. 39, no. 2, pp. 615–623.
- Gómez, R & Castro, R 2022b, 'Stress modelling using cellular automata for block caving applications', *International Journal of Rock Mechanics and Mining Sciences*, vol. 154, [https://authors.elsevier.com/sd/article/S1365-1609\(22\)00091-0](https://authors.elsevier.com/sd/article/S1365-1609(22)00091-0)
- Gustafsson, P 1998, *Waste Rock Content Variations During Gravity Flow in Sublevel Caving*, Luleå University of Technology, Luleå.
- Hancock, W 2013, *Gravity Flow of Rock in Caving Mines : Numerical Modelling of Isolated, Interactive and Non-Ideal Draw*, The University of Queensland, Brisbane.
- Hashim, M 2011, *Particle Percolation in Block Caving Mines*, PhD thesis, The University of New South Wales, Sydney.
- Jenike, AW, Johanson, JR & Carson, JW 1973, 'Bin Loads—Part 3: Mass-Flow Bins', *Journal of Engineering for Industry*, vol. 95, no. 1, pp. 6–12.
- Jimenez, O 2020, *Modelación Numérica de La Fragmentación Secundaria En Minería de Caving a Través de DEM*, Universidad de Concepción, Concepción.

- Jolley, D 1968, 'Computer simulation of the movement of ore and waste in an underground mining pillar', *The Canadian Mining and Metallurgical Bulletin*, vol. 61, no. 675, pp. 854–859.
- Killion, ME 1985, 'Design pressures in circular bins', *Journal of Structural Engineering*, vol. 111, no. 8, pp. 1760–1774.
- Kvapil, R 1965, 'Gravity flow of granular materials in hoppers and bins - Part I', *International Journal of Rock Mechanics and Mining Sciences*, vol. 2, no. 1, pp. 35–41.
- Kvapil, R 2008, *Gravity Flow in Sublevel and Panel Caving*, Luleå University of Technology Press, Luleå.
- Langston, PA, Tüzün, U & Heyes, DM 1995, 'Discrete element simulation of internal stress and flow fields in funnel flow hoppers', *Powder Technology*, vol. 85, no. 2, pp. 153–169.
- Laubscher, DH 1994, 'Cave mining - the State of the Art', *Journal of the Southern African Institute of Mining and Metallurgy*, vol. 94, no. 10, pp. 279–293.
- Laubscher, DH 2000a, *Block Cave Manual*, Julius Kruttschnitt Mineral Research Centre, The University of Queensland, Brisbane.
- Laubscher, DH 2000b, 'Dilution', *Block Cave Manual*, prepared for the International Caving Study (1997-2000), Julius Kruttschnitt Mineral Research Centre, and Itasca Consulting Group, Brisbane.
- Hashim, MHM, Sharrock, GB & Saydam, S 2008, 'A review of particle percolation in mining', in Y Potvin, J Carter, A Dyskin & R Jeffrey (eds), *SHIRMS 2008: Proceedings of the First Southern Hemisphere International Rock Mechanics Symposium*, Australian Centre for Geomechanics, Perth, pp. 273–284, [https://doi.org/10.36487/ACG\\_repo/808\\_72](https://doi.org/10.36487/ACG_repo/808_72)
- Mahmoodi, F 2012, 'Compression mechanics of powders and granular materials probed by force distributions and a micromechanically based compaction equation', doctoral dissertation, Uppsala University, Uppsala.
- Michot-Roberto, S, Garcia-Hernández, A, Dopazo-Hilario, S & Dawson, A 2021, 'The spherical primitive and perlin noise method to recreate realistic aggregate shapes', *Granular Matter*, vol. 23, no. 2, <https://doi.org/10.1007/s10035-021-01105-6>
- Olivares, D, Castro, R, & Hekmat, A, 2015, 'Influence of fine material, humidity and vertical loads on the flowability of caved rock', *Proceedings of the 49th U.S. Rock Mechanics/Geomechanics Symposium*, American Rock Mechanics Association, Alexandria.
- Orellana, LF 2012, *Evaluación de Variables de Diseño Del Sistema de Minería Continua a Partir de Experimentación En Laboratorio*, Universidad de Chile, Santiago.
- Orellana, M, Cifuentes, C & Díaz, J 2014, 'Caving Experiences in Esmeralda Sector, El Teniente Mine' in R Castro (ed), *Caving 2014: Proceedings of the 3rd International Symposium on Block and Sublevel Caving*, Universidad de Chile, Santiago, pp. 78–90.
- Pierce, ME, Cundall, PA, Van Hout, G & Lorig, L 2017, 'PFC 3D modeling of caved rock under draw', *Numerical Modeling in Micromechanics via Particle Methods*, pp. 211–217.
- Pierce, ME 2019, 'Forecasting vulnerability of deep extraction level excavations to draw-induced cave loads', *Journal of Rock Mechanics and Geotechnical Engineering*, vol. 11, no. 3, pp. 527–534, <https://doi.org/10.1016/j.jrmge.2018.07.006>
- Pierce, ME 2009, *A Model for Gravity Flow of Fragmented Rock in Block Caving Mines*, PhD thesis, The University of Queensland, Brisbane.
- Power, G 2004, 'Full scale SLC draw trials at Ridgeway gold mine', in A Karzulovic & M Alfaro (eds), *Proceedings of Massmin 2004*, Instituto de Ingenieros de Chile, Santiago, pp. 225–230.
- Sahupala, H, Brannon, C, Annavarapu, S & Osborne, K 2008, 'Recovery of extraction pillars in the Deep Ore Zone (DOZ) block cave, PT Freeport Indonesia', in H Schunnesson & E Nordlund (eds), *MassMin 2008: Proceedings of the 5th Conference and Exhibition on Mass Mining*, Luleå University of Technology, Luleå, pp. 191–202.
- Sánchez, V, Castro, RL & Palma, S 2019, 'Gravity flow characterization of fine granular material for block caving', *International Journal of Rock Mechanics and Mining Sciences*, vol. 114, pp. 24–32, <https://doi.org/10.1016/j.ijrmms.2018.12.011>
- Sperl, M 2006, 'Experiments on corn pressure in silo cells - translation and comment of Janssen's paper from 1895', *Granular Matter*, vol. 8, no. 2, pp. 59–65.
- Steffen, S & Kuiper, P 2014, 'Case study: improving SLC recovery by measuring ore flow with electronic markers', in R Castro (ed), *Caving 2014: Proceedings of the 3rd International Symposium on Block and Sublevel Caving*, Universidad de Chile, Santiago, pp. 328–336.
- Sun, H, Gao, Y, Elmo, D, Jin, A, Wu, S & Dorador L 2019, 'A study of gravity flow based on the upside-down drop shape theory and considering rock shape and breakage', *Rock Mechanics and Rock Engineering*, vol. 52, no. 3, pp. 881–893, <http://dx.doi.org/10.1007/s00603-018-1514-1>
- Susaeta, A 2004, 'Theory of gravity flow (part 1)', in A Karzulovic & M Alfaro (eds), *Proceedings of Massmin 2004*, Instituto de Ingenieros de Chile, Santiago, pp. 167–172.
- Torres, C 2019, *Rate of Draw Effect on Fragmentation*, Santiago.
- Vallejos, J, Basaure, K, Palma, S, & Castro, R 2017, 'Methodology for evaluation of mud rush risk in block caving mining', *Journal of the Southern African Institute of Mining and Metallurgy*, vol. 117, no. 5, pp. 491–497.
- Vergara, P 2016, *Estudio Experimental de Flujo Gravitacional En Minería de Panel Caving*, Universidad de Chile, Santiago.
- Viera, E & Diez, E 2014, 'Analysis of hang-up frequency in Bloque 1–2, Esmeralda Sur Mine', in R Castro (ed), *Caving 2014: Proceedings of the 3rd International Symposium on Block and Sublevel Caving*, Universidad de Chile, Santiago, pp. 138–145.